

Electronic Supplementary Information

Large temperature tuning of emission color of a phosphor by dual use of Raman and Photoluminescence signals

Arnab De and Rajeev Ranjan*

Department of Materials Engineering, Indian Institute of Science, Bangalore-560012, India

*rajeev@iisc.ac.in

Experimental Details

Specimens of Eu (0.5 mol%) doped BaTiO₃ (BT:0.5Eu), Er (0.5 mol%) doped BaTiO₃ (BT:0.5Er) and Eu, Er codoped BaTiO₃ were prepared by conventional solid state synthesis route. Stoichiometric amounts of dried high purity chemicals BaCO₃ (99.8%, Alfa Aesar), TiO₂ (99.8%, Alfa Aesar), SnO₂ (99.9%, Alfa Aesar), Eu₂O₃ (99.9%, Alfa Aesar) were thoroughly mixed in Zirconia Vials and balls in acetone medium using planetary ball mill (P5) for 10-12 hour at rotating speed of 150 rpm. The milled powders were dried and calcined at 1120 °C in alumina crucible for 4 hours. Sintering was carried out at 1350 °C for 4 hour. Eu (0.5 mol%) doped SrTiO₃ (STO:0.5Eu) ceramics have been prepared starting with SrCO₃ (99.8%, Alfa Aesar) at a calcination temperature 1000°C for 4 hour and sintering temperature 1300°C for 4 hour. Eu (0.5 mol%) doped BaZrO₃ (BZO:0.5Eu) and Er (0.5 mol%), Eu (0.5 mol%) co-doped BaZrO₃ (BZO:0.5Er0.5Eu) ceramics were prepared using BaCO₃(99.8%, Alfa Aesar) ZrO₂ (99.8%, Alfa Aesar) by calcining at 1250°C for 4 hour and sintering temperature 1500°C for 6 hours. All emission spectroscopy data were collected using 532 nm laser attached with LabRAM HR (HORIBA) spectrometer coupled with CCD detection system. All Experiments were carried out in a backscattering configuration with a laser spot size of ~ 7 μm under a 10x microscope and 3 s acquisition time. The CIE (x,y) color coordinates were calculated from emission spectra using color calculator by OSRAM SYLVANIA. The time resolved experiments (life time measurement) were performed in Edinburgh Instruments (Model : uF920H) using pulse light source (width : 1.5 - 2.5 μs) with repetition rate of 100Hz. Measurements were carried by excitation wave-length of 532 nm, monitoring emission at 595 nm for Eu³⁺ and 552 nm for Er³⁺.

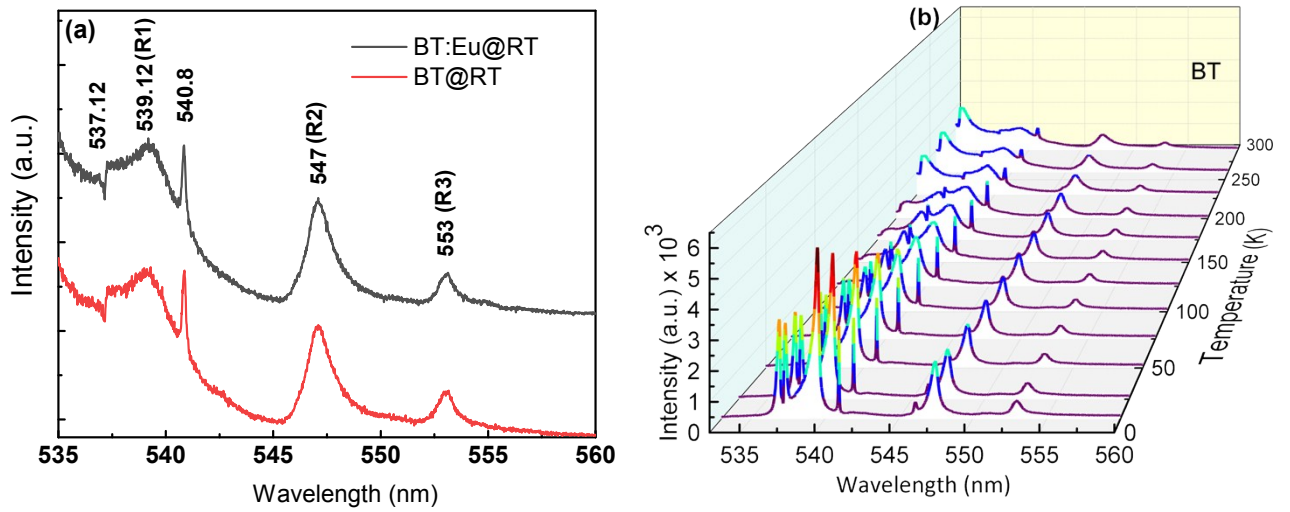


Fig. S1 a) Room Temperature emission spectra of Eu doped and undoped BT in lower wavelength region (in wavelength range 535-560 nm). In this region the spectrum is primarily because of Raman scattering. b) Temperature dependence of the emission spectra of BT in lower wavelength region.

TABLE S1. Room Temperature Raman modes (with phonon assignments) of BaTiO₃ polycrystalline specimen in nm scale and the corresponding Raman shift in cm⁻¹.

Phonon Assignments	Peak position in nm in the emission spectra	Peak position in cm ⁻¹ as Raman shift
A ₁ (TO)	539.18	248.25
B ₁ , E(TO + LO)	540.8	305.87
A ₁ , E(TO)	547	515.45
A ₁ , E(LO)	553	713.81

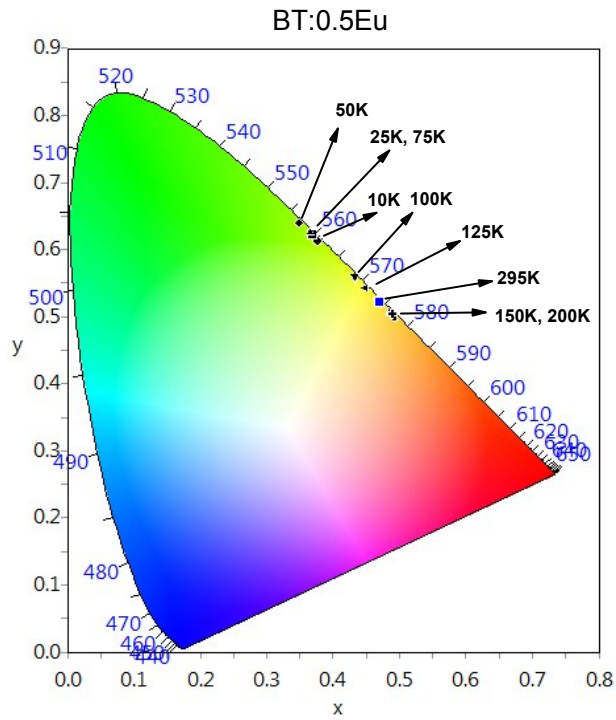


Fig. S2 Commission Internationale d'Eclairage (CIE) chromaticity diagram showing the temperature dependence of color coordinates (x,y) of BT:0.5Eu. Note that the color coordinates varies in a non-monotonic manner in the temperature intervals 10 K- 75 K and 150 K- 295 K.

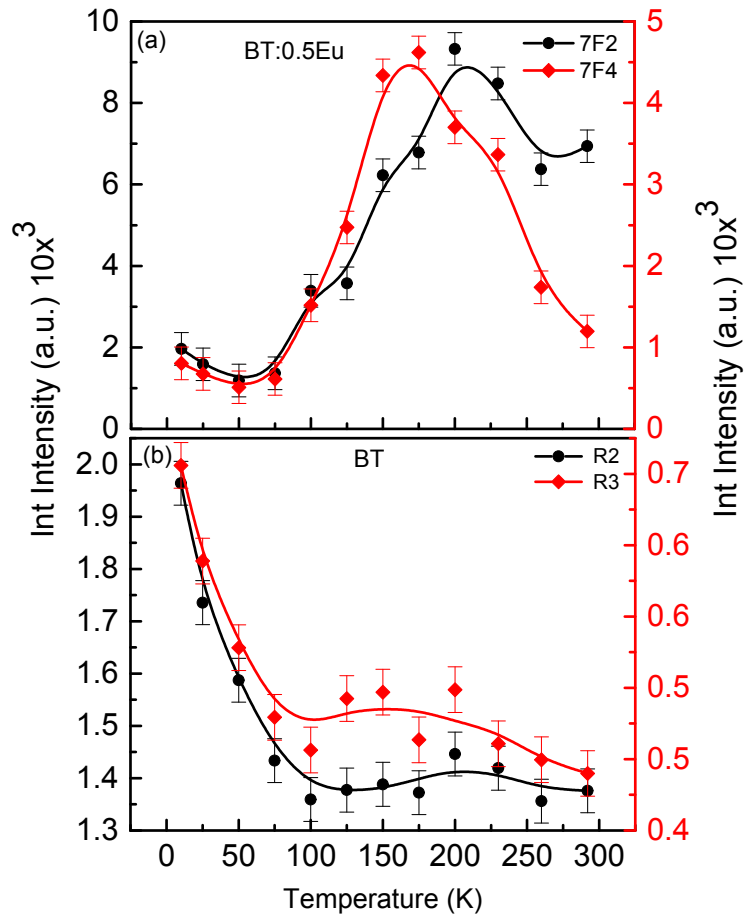


Fig. S3 a) Temperature dependence of the integrated intensity of the different Eu^{3+} PL bands (${}^5D_0 \rightarrow {}^7F_2, {}^7F_4$) of BT:0.5Eu. b) The temperature dependence of the integrated intensity of the Raman modes R2 (545-549.5 nm) and R3 (551.8-554.4 nm)) of BT.

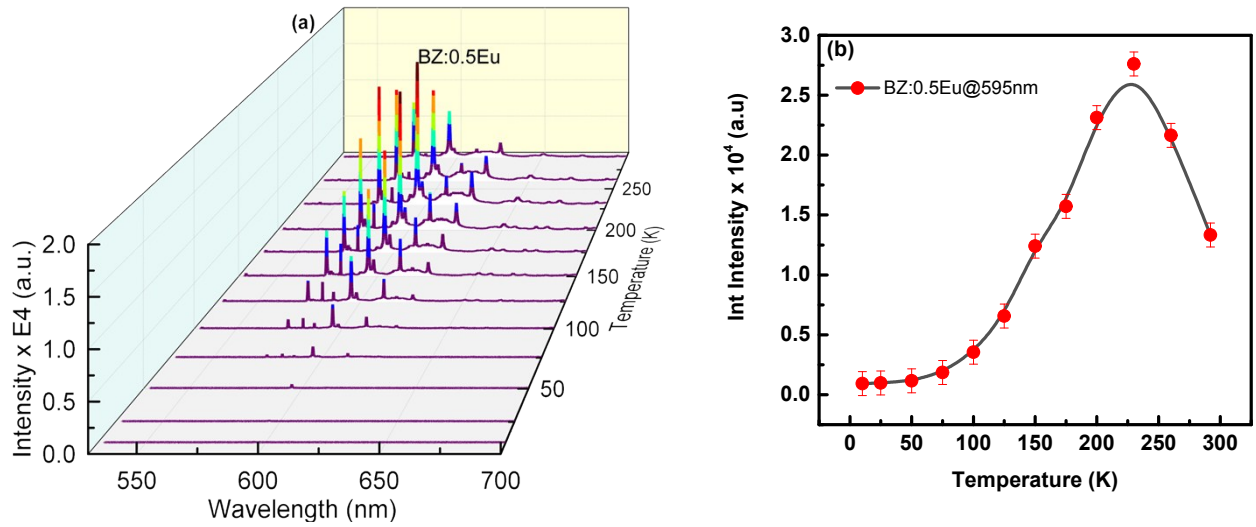


Fig. S4 a) Temperature dependence of the emission spectra of 0.5 mol% Eu doped BaZrO₃. b) Temperature evolution of the integrated intensity of the Eu³⁺ ⁷F₁ stark band (at \square 595 nm) of BZ:0.5Eu.

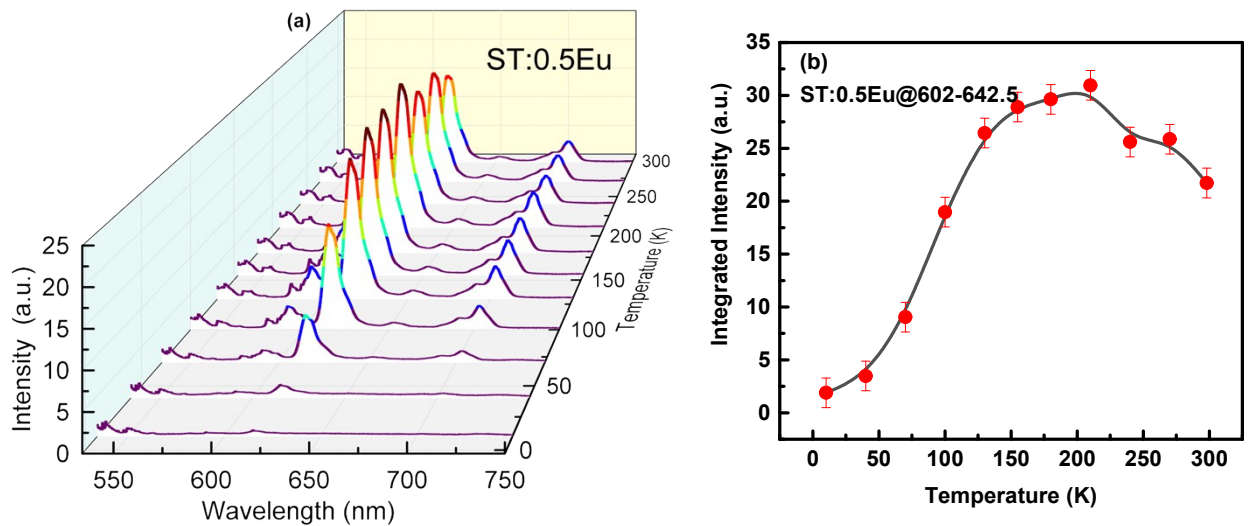


Fig. S5 a) Temperature dependence of the emission spectra of 0.5 mol% Eu doped SrTiO₃. b) Shows the temperature evolution of the integrated intensity of Eu³⁺ ⁷F₂ stark band (at \square 620 nm).

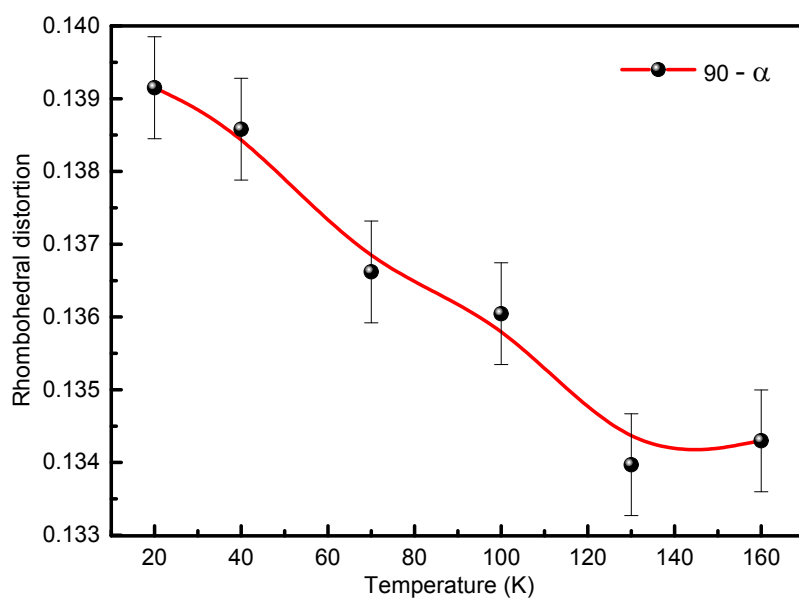


Fig. S6 Temperature dependence of the rhombohedral distortion angle ($90 - \alpha$; where α is the rhombohedral angle) of BT:0.5Eu for the temperature region of 160 K to 20 K.

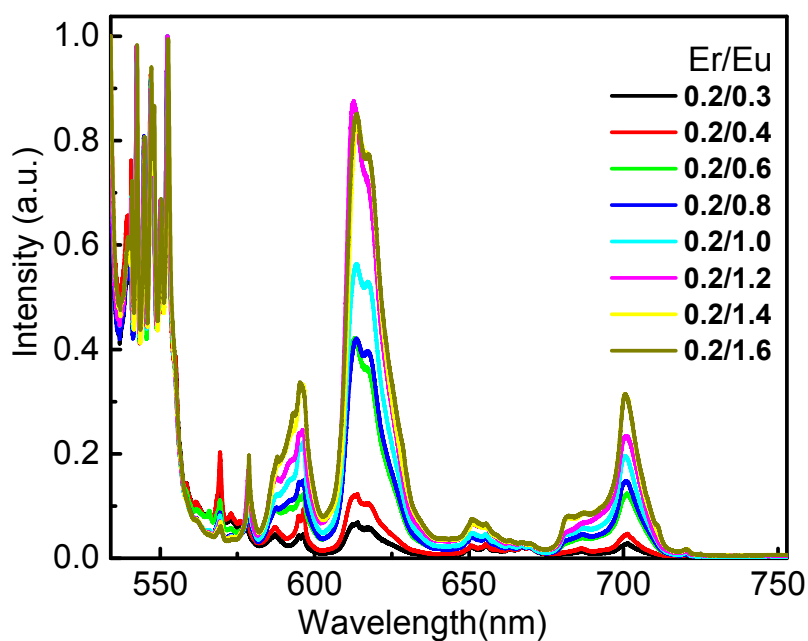


Fig. S7 Evolution of emission spectra on a normalized scale of Er and Eu co-doped BT with varying Eu concentration from 0.3 to 1.6 mol% keeping the Er concentration fixed at 0.2 mol%.

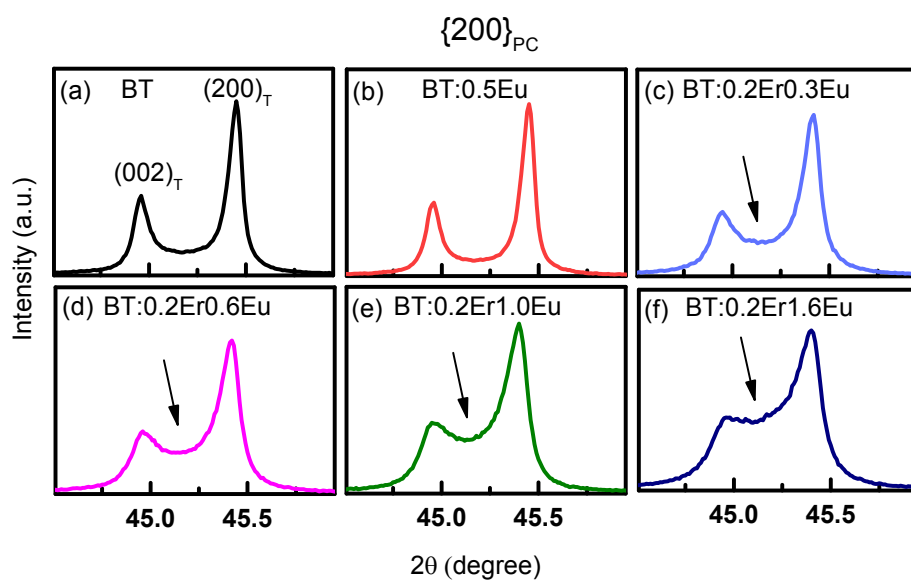


Fig. S8 Pseudo cubic $\{200\}_{PC}$ Bragg profile of powder specimen of (a) pure BT (b) 0.5 mol% Eu doped BT and (c)-(f) Er, Eu co-doped BT specimens with varying Eu concentration (0.3, 0.6, 1.0 and 1.6 mol%) keeping the Er concentration fixed at 0.2 mol%. doping of Eu on BaTiO₃ does not have any influence on the tetragonal ($P4mm$) crystal lattice of the host. Whereas co doping of Er and Eu affects the crystal lattice by inducing new phase (intensity enhancement indicated by arrow in between $(200)_T$ and $(002)_T$ peaks) and this phase increases with increasing Eu^{3+} concentration.

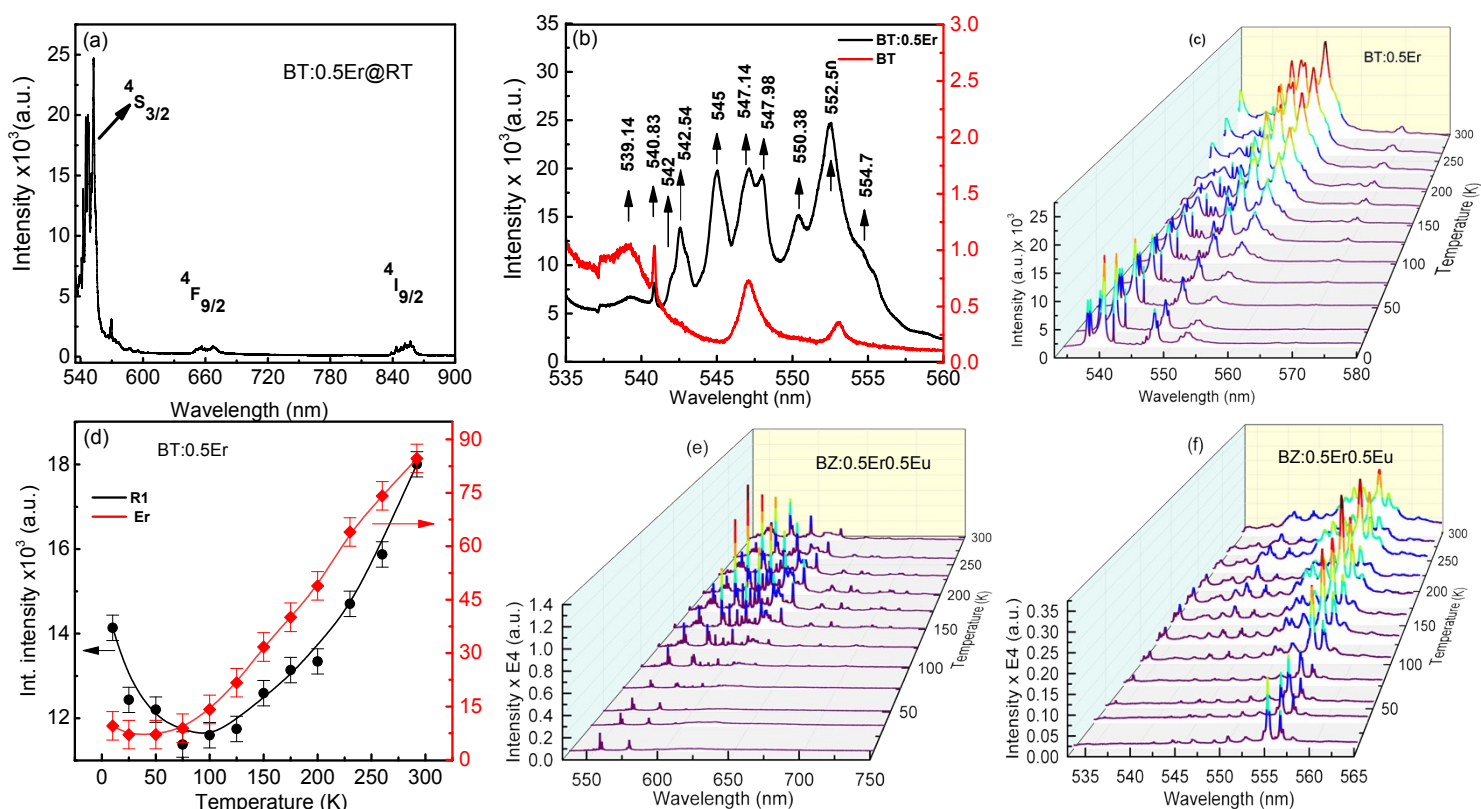


Fig. S9 a) Room temperature emission spectra of 0.5 mol % Er doped BaTiO₃. b) Comparison between the room temperature emission spectra of Er doped and undoped BaTiO₃ in the green region. Here the Er PL bands overwhelms the Raman bands. c) Temperature evolution of the emission spectra of BT:0.5Er (in the green region). d) Temperature dependence of the integrated intensities of the emission peaks at \square 539 nm and \square 552.5 nm of BT:0.5Er. e) Temperature dependence of the emission spectra of 0.5 mol% Eu and 0.5 mol% Er co-doped BaZrO₃. f) Highlights the temperature evolution in the green region (arising from Er³⁺ PL emission) of BZ:0.5Er0.5Eu. Note that the Eu³⁺ PL intensity decreases dramatically on cooling below 200 K. The intensity of Er³⁺ PL also decreases but not as dramatically as for the Eu³⁺.

The PL bands of the Er-doped specimens are observed in the green (535-565 nm), red (640-680 nm) and near-IR (830-870 nm) regions, and correspond to $^4S_{3/2} \rightarrow ^4I_{15/2}$, $^4F_{9/2} \rightarrow ^4I_{15/2}$, and $^4I_{9/2} \rightarrow ^4I_{15/2}$, transitions respectively¹². The intensity of the strong green Er³⁺ PL band lies exactly in the wavelength region where Raman modes of BaTiO₃ appear. Figure S5(b) shows a comparison of the emission spectra of pure BT and BT:0.5Er in the wavelength region 535 – 560 nm, measured under identical condition (laser power, acquisition time and the focusing lens). The spectrum of BT:0.5Er at 300 K comprise of superposed PL + Raman bands at 542, 542.54, 545, 547.14, 547.98, 550.38, 552.50 and 554.7 nm¹. The Raman bands of BaTiO₃ are separately visible at only at 540.83 nm [B₁, E (TO + LO)]

and 539.14 nm [$A_1(TO)$]. Important to note that the peak intensity of the R1 band of BT:5Er (at 539 nm) is more than 5 times than for undoped BT, suggesting that the overall enhancement of the green intensity is in part contributed by Er-doping also increasing the Raman scattering cross-section of the host BaTiO₃.

In contrast to the intensity trend of the strongest Eu⁺³ PL, which shows a maximum at ~200 K (main text Figure 1c), the intensity of the Er⁺³ strongest PL band ($^4S_{3/2} \rightarrow ^4I_{15/2}$) at 552.50 nm decreases monotonously below 300 K (Figure S5(c)). The intensity of the R1 band of Er-doped BT also decreases continuously on cooling down to 100 K (Figure S5(d)) and increases below 100K. The monotonic decrease of the Er PL intensity on cooling was also found in Er and Eu co-doped BaZrO₃, an ideal cubic perovskite exhibiting no first order Raman modes, (Figure S5 (e) and (f)) confirming that this tendency is not primarily related to the ferroelectric nature of the host BaTiO₃. We may point out that in comparison to Eu⁺³ PL, the intensity of which is attenuated by ~ 96 % at 10 K, the Er⁺³ PL band is less attenuated (intensity reduced by ~ 65 %).

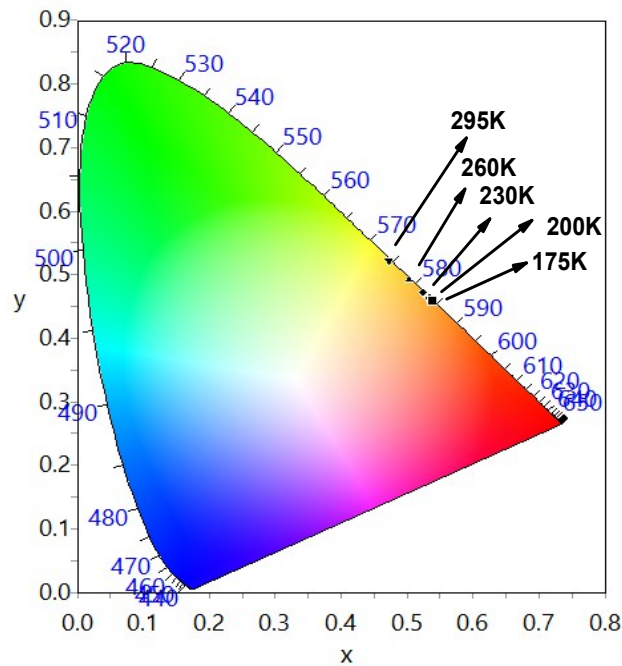


Fig. S10. Temperature dependence of CIE color coordinates (x,y) of BT:0.2Er1.6Eu in the temperature range 175 K- 295 K(varies between red and yellow).

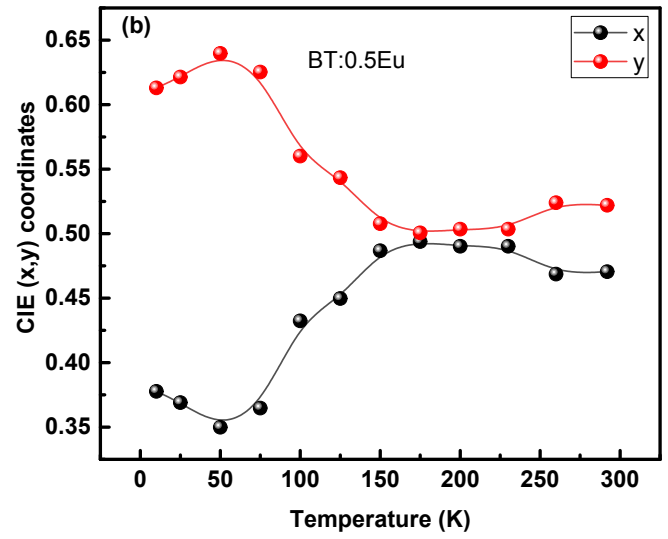
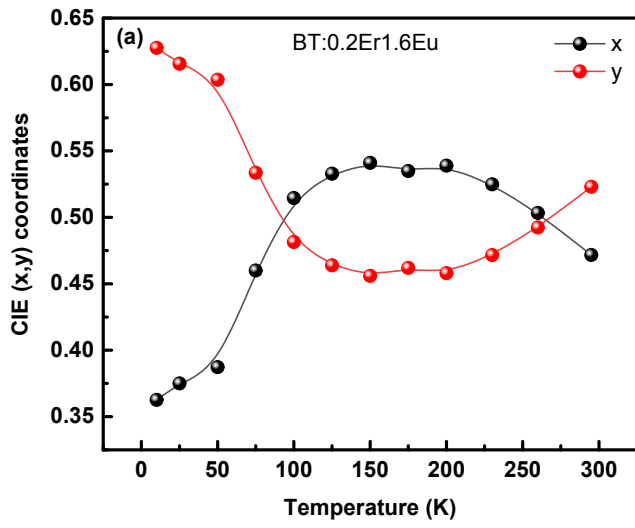


Fig. S11 a,b) Temperature dependence of CIE color coordinates (x,y) of BT:0.2Er1.6Eu and BT:0.5Eu. The co-doped specimen shows a maximum change of (x,y) coordinates $|\Delta x| \approx |\Delta y| = 0.18$ in the temperature range 10 K-150 K. The corresponding change for BT:0.5Eu is $|\Delta x| \approx |\Delta y| = 0.11$.

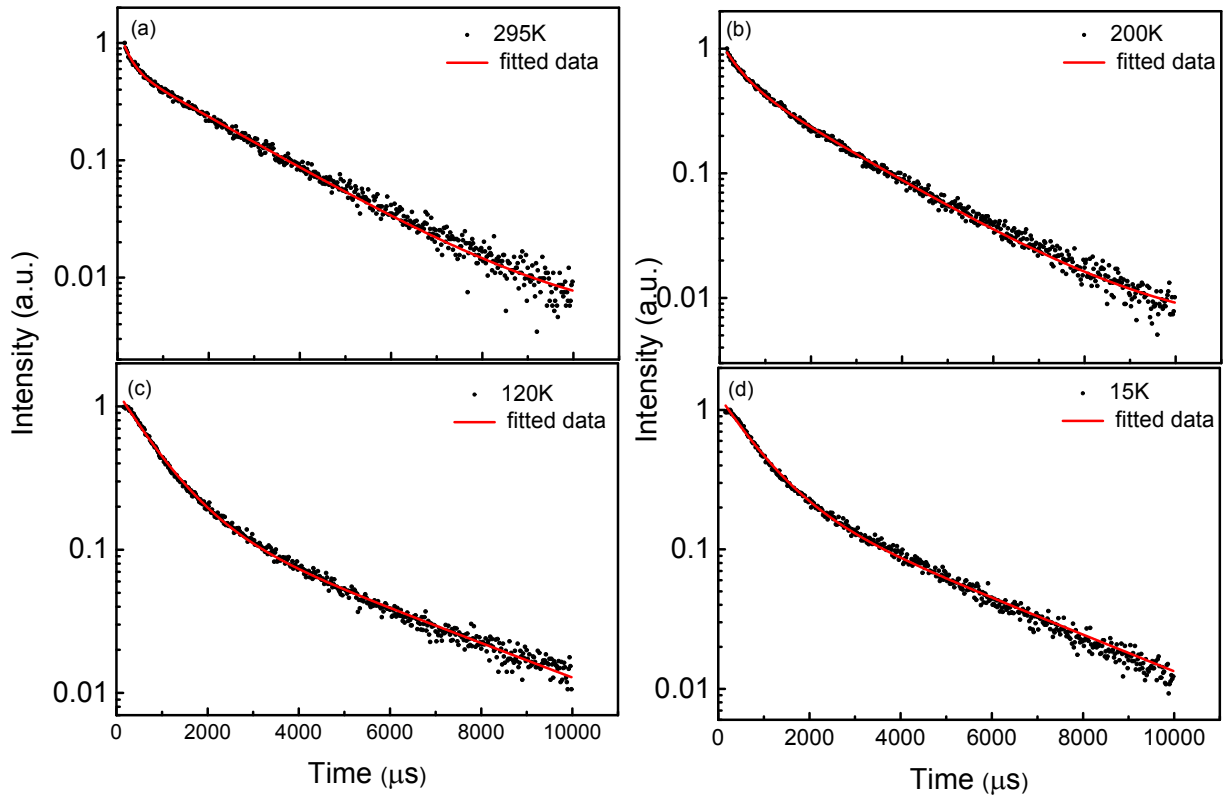


Fig. S12 Photoluminescence decay time profiles of Eu^{3+} in BT:0.5Eu (at λ 595 nm) at different temperatures a) 295K, b) 200K, c) 120K, d) 15K. The decay profiles are fitted satisfactorily with biexponential model (see text).

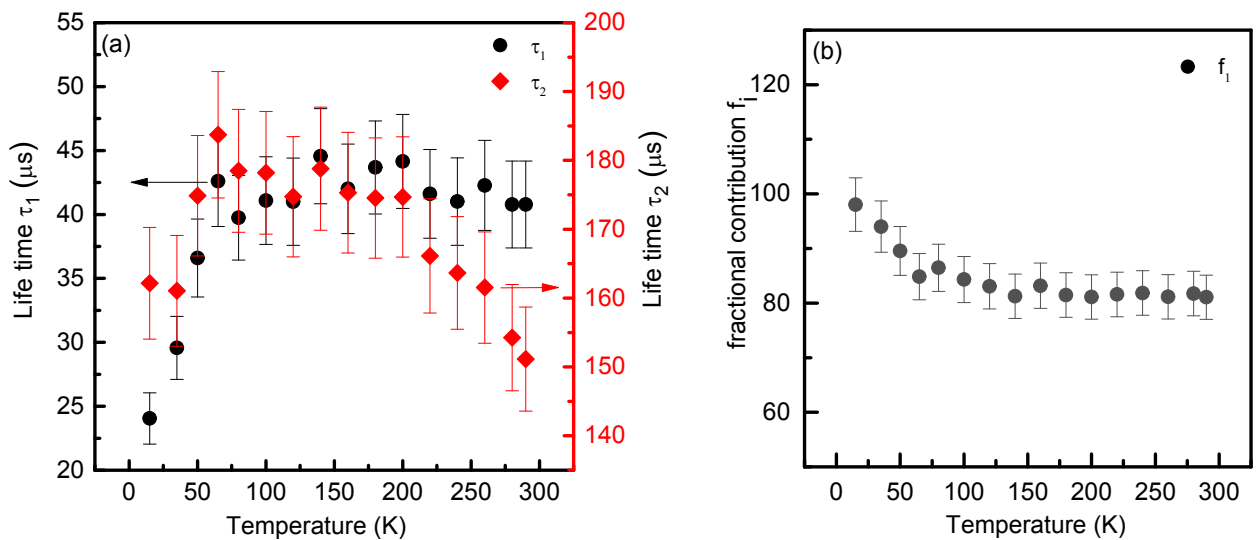


Fig. S13 a) Temperature dependence of lifetimes (τ_1 shorter lifetime and τ_2 longer lifetime) of the Er^{3+} (at λ 552 nm) of BT:0.5Er. b) Temperature dependence of the fractional contribution of the process corresponding to the shorter lifetime (f_1) to the steady state intensity.

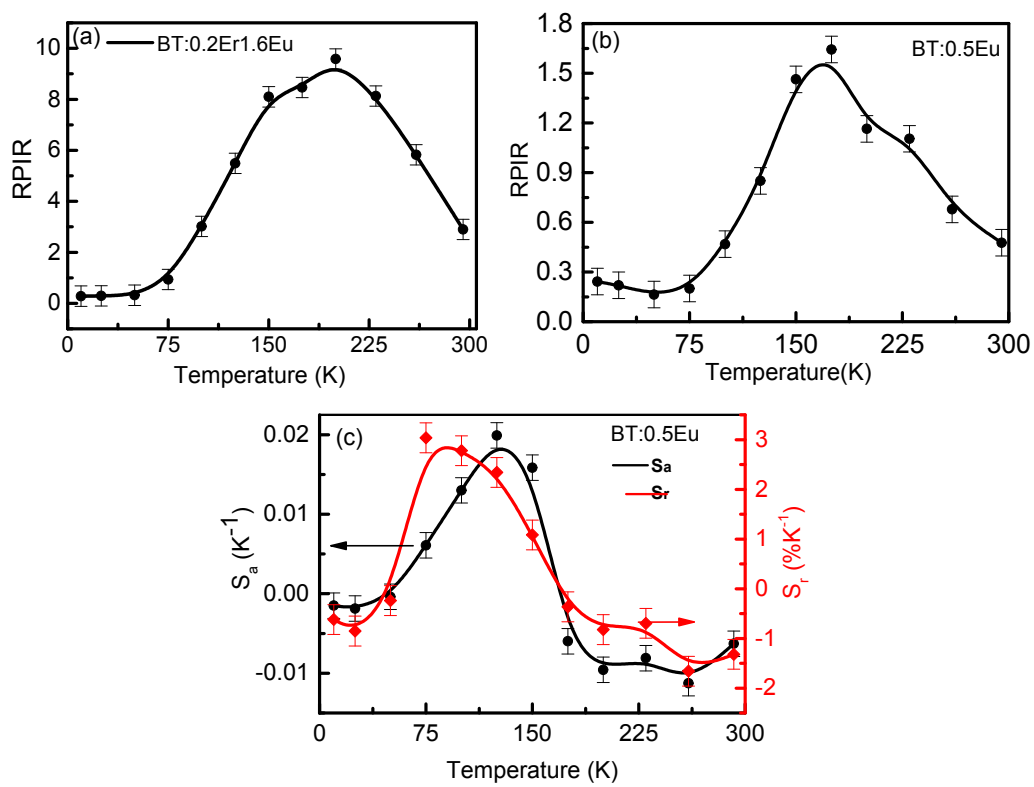


Fig. S14 Temperature dependence of Raman Photoluminescence Intensity Ratio of (a) BT:0.2Er1.6Eu and (b) BT:0.5Eu considering emission peaks at λ 539 nm (R1) and at λ 705 nm ($^5D_0 \rightarrow ^7F_4$). (c) Temperature dependence of Absolute and Relative sensitivity (S_a and S_r) of BT:0.5Eu.

References

- 1 D.-Y. Lu, W. Cheng, X.-Y. Sun, Q.-L. Liu, D.-X. Li and Z.-Y. Li, Abnormal Raman spectra in Er-doped BaTiO₃ ceramics, *J. Raman Spectrosc.*, 2014, **45**, 963–970.
- 2 D. Manzani, J. F. D. S. Petrucci, K. Nigoghossian, A. A. Cardoso and S. J. L. Ribeiro, A portable luminescent thermometer based on green up-conversion emission of Er³⁺/Yb³⁺ co-

doped tellurite glass, *Sci. Rep.*, 2017, **7**, 41596.